Avani Kumar Upadhyay[1], Manjeet Singh Goyat[2]*,
Ajay Kumar[2], Rashi Nathawat[3]

[1]*Department of Mechanical Engineering, School of Engineering, University of Petroleum and Energy Studies Dehradun, Uttarakhand, India,* [2]*Department of Applied Science, School of Engineering, University of Petroleum and Energy Studies Dehradun, Uttarakhand, India,* [3]*Functional Ceramics and Smart Materials Lab, Department of Physics, Manipal University Jaipur, Rajasthan, India*

Taguchi design of experiments based optimization and experimental investigation of mechanical performance of hybrid epoxy nanocomposites

ABSTRACT

The rising demand of safety in the aerospace and automobile industry is continuously motivating researchers to develop high strength, lightweight hybrid polymer composites, usually consisting a combination of carbon nanotubes (CNTs) and ceramic nanoparticles in the epoxy matrix. However, the development of such composites are usually hindered by some existing challenges, such as optimization of the concentration of CNTs, nanoparticles and their distribution in viscous epoxy matrices. In order to make the most of the impressive mechanical characteristics of CNTs and SiO_2 nanoparticles, ultrasonic dual mixing (UDM) technique was employed to develop $MWCNT/SiO_2$ based hybrid epoxy nanocomposites (HENCs). A well-known approach, such as the Taguchi design of experiment, was used to optimize the concentration of MWCNT, SiO_2 nanoparticles in epoxy and curing cycle of epoxy with respect to the tensile strength of the resulting HENCs. Additionally, the tensile strength, Young's Modulus, Strain to failure, and hardness were measured for HENCs. The results revealed that the optimal concentration of 1% MWCNT and 10% SiO_2 leads to the maximum increase in tensile strength and other mechanical properties of the HENCs.

Keywords: *hybrid nanocomposite, ultrasonic dual mixing, optimization, micromechanics, epoxy, Mechanical properties*

1. INTRODUCTION

Lightweight polymer nanocomposites with appropriate functional qualities are of great interest in developing structural engineering materials for a broad range of applications. Applications for polymers based on the thermoset epoxides include adhesives, coatings, sporting equipment (such as rackets, helmets, sticks, and skis), aerospace, and automotive industries. The exceptional performance of cross-linked polymers (epoxy) under different loading conditions has led to their widespread use [1]. Epoxy possesses remarkable mechanical and physical qualities, including high strength, little shrinkage, and high resistance to heat and chemicals [2-4].

A strongly cross-linked network, on the other hand, provides a brittle character to epoxy, indicating weak resistance of epoxy to avoid fracture propagation, causing low toughness of the final product [5,6]. The distribution of nanoparticles into the epoxy matrix and filler-matrix interfacial bonding are the two primary factors that significantly control the tensile strength and fracture toughness of the resulting nanocomposite. A variety of nanofillers such as TiO_2, Al_2O_3, SiO_2, Fe_2O_3, ZrO_2, Multiwall carbon nanotubes (CNTs), and graphene were used in the past to increase the toughness of the nanocomposites [7-12]. There have been a plethora of studies published over the past decade examining the behaviour of CNTs reinforced polymer composites subjected to different kinds of loads and implemented in a variety of polymer matrices. CNTs are well-known for improving the electrical, mechanical, morphological, and thermal properties of epoxy nanocomposites [13,14]. Because the CNTs offer

extraordinary strength and rigidity, which enhance the mechanical properties of the polymer nanocomposites [15,16]. The cluster-free distribution of Multi-walled CNTs (MWCNTs) in a polymer and their interfacial interaction with the base matrix are the two most critical parameters that determine the effectiveness of CNTs in polymer nanocomposites [17]. The fabrication of high-performance polymer nanocomposites is complicated by the difficulty of ensuring homogeneous distribution and virtuous interfacial contact of CNTs with the adjoining epoxy matrix. The immense specific surface area of CNTs causes them to entice one another sturdily, resulting in the development of clusters owing to the van der Waals forces [18]. Functionalizing CNTs via chemical processes is a key strategy for addressing the aforementioned issues [19]. However, the functionalization disrupts the CNTs' atomic arrangement and creates defects, both of which lower the nanocomposite's performance [20, 21]. Other non-chemical modification techniques like ultrasonic dual mixing (UDM), shear mixing and hybridization can also be used to solve the clustering problem of CNTs. UDM is the most effective method for dispersing CNTs uniformly across a matrix because it combines high-frequency ultra-sonication mixing with an axial flow impeller. The hybridization, in which oxide nanoparticles (ONPs) and MWCNT are simultaneously mixed into a pristine epoxy base to improve CNT particle distribution, is a novel strategy. The oxide nanoparticles combined with carbon nanotubes (CNTs) in an epoxy matrix not only slow down the crack's progression but also act as a spacer to lessen the attraction force between the CNTs [22-24]. Nanosized SiO_2 particles are commonly utilised as fillers in polymer composites, because of their various beneficial characteristics such as non-toxicity, low cost, chemical inertness, biocompatibility, ability to reinforce and thermal resistance [25,26].

In order to combine the desirable characteristics of SiO_2 particles (crystallinity, hardness, thermal stability, and stiffness), researchers have demonstrated a strong interest in incorporating SiO_2 particles into the MWCNT/epoxy composite. The influence of SiO_2 nanoparticles on CNT shape and characteristics was studied by He et al. [27]. They found that MWCNT's strength is improved (≥ 200%) by silica addition. The morphology of MWCNT with additional silica is like a human spine, with numerous projections. In addition, the silica particles provide protection to the surface of CNT, making it thermally stable. The mechanical properties of the hybrid silica-CNT-epoxy composite were compared to those of nanocomposites based on the individual components by Xiao et al. [28]. The hybrid nanocomposites exhibited superior properties. The mechanical and tribological performance of hybrid Silica-MWCNT-Acrylic silicon nanocomposite was studied by Zhou et al. [29]. The hardness and tribological performance of the nanocomposite with 2.0wt.% hybrid material was the highest. Alansari et al. [30] studied the theoretical model fitness for finding the tensile modulus of SiO_2-TiO_2-epoxy nanocomposite. The researcher reported that the Halpin-Tsai model is in good agreement with the practical results. Though researchers have tried to develop MWCNT-SiO_2-epoxy hybrid polymer nanocomposite (MPNC), limited efforts have been made to achieve the optimum particle concentration and curing cycle to maximize the mechanical performance of nanocomposite.

In the present study, hybrid epoxy nanocomposites (HENCs) were developed by incorporating a varying weight percentage of MWCNT/SiO_2. The HENCs were developed using an optimized UDM process [4]. Taguchi design of experiments was performed to optimize the concentration of MWCNT, SiO_2 nanoparticles in epoxy and curing cycle of epoxy with respect to the tensile strength of the HENCs. The mechanical properties of HENCs are significantly improved at an optimal concentration of 1% MWCNT and 10% SiO_2 nanoparticles.

2. MATERIALS AND METHODS

2.1. Materials

Multi-walled carbon nanotubes (MWCNTs) with an average diameter of 20 nm and SiO_2 nanoparticles with an average diameter of 15 nm (spherical shape) were used as nanofillers. The MWCNTs and SiO_2 nanoparticles were purchased from Reinste Nano Venture ltd. Delhi, India. The epoxy polymer, which was used as a matrix procured from Fine, finish organic Pvt. Limited (India). The epoxy comprises Epofine-557 (medium viscosity laminating grade multifunctional liquid epoxy resin) and Finehard-5200 aromatic amine hardener. The epoxy used in the current study is a typical material used in bulk, especially in the automotive and aerospace industries [31]. Typical physical properties of the epoxy system reported by the manufacturer are shown in Table 1. Common solvents like acetone and methyl ethyl ketone (MEK) were procured from Sigma Aldrich, India.

Table 1. Typical properties of epoxy system

Tabela 1. Tipične osobine epoksidnog sistema

Material	Viscosity at 25°C (mPas)	Density at 25 °C (g/cm3)	Flash Point (°C)	Storage Life (years)
Epofine-557	25000-40000	1.15-1.12	>200	3
Finehard-5200	140-200	0.99-1.02	>120	1

2.2. Preparation of hybrid nanocomposite

Dispersing nanoparticles in a viscous epoxy resin via sonication necessitates an energy level high enough to break up nanoparticle clusters. At the same time, it needs to be quick enough so that the pristine epoxy does not lose its molecular structure. Ultrasonic horns dipped into epoxy resin generate localised heat during UDM, which can compromise base material qualities. A number of factors, including pulse-on time, sonication time, pulse-off time, material volume, sonication amplitude and stirring speed, contribute to the localised heat generation during UDM. Therefore, MEK solvent was mixed into the epoxy, which not only worked as a coolant but also diminished the viscosity of the base epoxy. In order to regulate the increase in temperature in the region of the ultrasonic horn, an automatic temperature control probe and an ice water bath were used to keep the resin/MEK combination at a constant 30 $^{\circ}$C throughout the process. The hybrid epoxy nanocomposite samples were prepared following the optimized UDM process parameters such as sonication time = 60 min, pulse on time = 10 min, amplitude = 80%, and stirrer speed = 500 rpm [2].

Hybrid nanocomposite samples were prepared by varying the concentration of MWCNTs (0.1 – 1 wt.%), SiO$_2$ nanoparticles (1 – 10 wt.%) and curing cycle (1 – 5) as per Taguchi L5 orthogonal array. These three parameters were varied up to 5 levels, as shown in Table 2. Compared to a full-factorial experiment, which would require 5^3 = 125 runs to evaluate three parameters at five levels, Taguchi's factorial experiment only requires 25 experiments. Signal to noise ratio (S/N) values was calculated by analysing the impact of three control variables on

the tensile strength of hybrid nanocomposite using the "larger-the-better" formula (Eq. 1) to determine the optimal arrangement of variables:

$$\frac{s}{n} = -10log\frac{1}{n}\sum_{i=1}^{n}\frac{1}{y_i^2} \quad n = 25 \qquad (1)$$

here, n = number of runs, y_i = ultimate tensile strength in the ith experiment (MPa).

Table 3 displays the results of an orthogonal L5 array with output in the form of the mean tensile strength of the hybrid epoxy nanocomposite.

A measured quantity of MEK (3 times the volume of epoxy) was introduced into the epoxy resin in order to decrease its viscosity. The resulting mixture was subsequently blended with SiO$_2$ and MWCNTs nanopowder at varying concentrations (as per Table 3), utilizing mechanical stirring by magnetic stirrer at 500 rpm for 30 min. Thereafter, the solution was UDM processed with optimized parameters. Subsequently, the MEK was extracted from the mixture by keeping the solution on a magnetic stirrer at 50 °C for 4 h. The MEK removal was confirmed by comparing the initial and final weights of the epoxy system (before and after adding the MEK). Then, a hardener was added in the ratio of 100:26 and hand stirring was applied for 20 min. The trapped air in the mixture during the mixing of hardener was removed using a high vacuum pump at 50 °C for 30 min. The mixture was introduced into iron moulds coated with Teflon tapes. Moulds were kept in the muffle furnace (Nabertherm make) for curing at different curing cycles. Samples were cleaned and dried properly after curing. Neat epoxy samples were also prepared at different curing cycles for the comparison of results.

Table 2. Variables or parameters and their levels used for the optimization

Tabela 2. Promenljive ili parametri i njihovi nivoi koji se koriste za optimizaciju

Parameter level ↓	MWCNT (wt%)	SiO$_2$ (wt%)	Curing cycle
1	0.1	1	120℃ / 2 h + 160℃ / 6 h (C1)
2	0.3	3	100℃ / 4 h + 120℃ / 2 h + 160℃ / 6 h (C2)
3	0.5	5	100℃ / 4 h + 120℃ / 2 h + 140℃ / 2 h + 180℃ / 2 h (C3)
4	0.7	7	140℃ / 4 h + 160℃ / 4 h + 180℃ / 2 h (C4)
5	1	10	160℃ / 2 h + 180℃ / 4 h + 200℃ / 4 h (C5)

2.3. Characterizations

The stress-strain curves were recorded as per ASTM D-638(V) using Computerized Tinius Olsen 50ST. A strain rate of 1 mm/min until rupture was used. The stress-strain curves were utilized to determine various mechanical properties such as tensile strength, elastic modulus (Young's modulus) and percentage of strain-to-break. The determination of the elastic modulus involves the computation of the ratio between the tensile stress and axial strain within the linear elastic region. The dimensions of the test samples were made according per the ASTM standard. At least 5 specimens were tested for each composition, and the mean values with standard deviations were reported.

Viker's hardness test was performed at 50 g force and a dwell time of 15 s. Tests were performed on Futurtech micro hardness tester by 120° diamond indenter. Specimens were mirror polished using appropriate grade emery paper and diamond paste polish before the hardness test. Hardness was measured at 10 randomly selected spots of all 5 specimens for each composition, and the average value with standard deviation was reported. MWCNTs and SiO_2 nanoparticles were dried in an oven at 100 ^{o}C for 2 h to remove the moisture content prior to their characterization. X-ray diffraction (XRD) analysis was performed on D8 ADVANCE ECO – Bruker having Cu-Kα radiation source (wavelength =1.54 Å). The test was performed at an accelerating voltage of 40 kV with an accelerating current of 20 mA, a step size of 0.05 scanning. Field emission scanning electron microscope (FESEM, JEOL, USA) analysis of MWCNTs and SiO_2 nanoparticles was performed at an accelerating voltage of 5 kV. Prior to FESEM analysis, the samples were dispersed in ethanol, poured on sample mounts, and allowed to dry at room temperature. The dried samples were gold-coated using a sputtering set up to obtain high quality images.

3. RESULTS AND DISCUSSION

3.1. Phase analysis and Morphology of MWCNT and SiO_2 nanoparticles

The XRD diffraction pattern of MWCNT and SiO_2 nanoparticles is shown in Fig. 1. The XRD pattern of MWCNT (Fig. 1a) shows clear, sharp peaks corresponding to the crystal planes of (002) and (100) at diffraction angles of 26° and 44°. The peaks correspond to a typical shape of a hexagonal graphitic structure. The diameter of MWCNT was determined using the Debye-Scherer equation (Eq. 2):

$$d = K \frac{\lambda}{\beta \cos \emptyset} \qquad (2)$$

where, d is the average diameter of crystallite, K is shape constant (0.9), λ is radiation wavelength (1.54 Å), β is full width at half maxima, $\emptyset$ is Bragg's angle of respective peaks. Using (Eq. 2), the crystallite size of MWCNT was found to be about 10 nm.

However, the XRD pattern of SiO_2 (Fig. 1b) peaks shows a typical nature of amorphous SiO_2 with no clear peaks, only a broad hump.
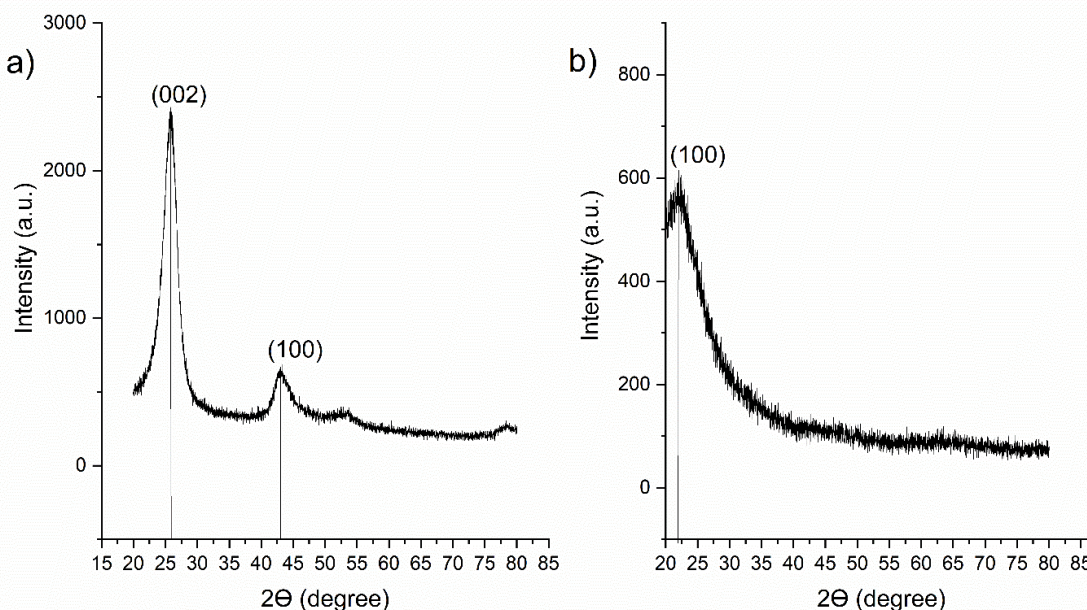

Figure 1. XRD pattern of (a) MWCNT and b) SiO_2 nanoparticles

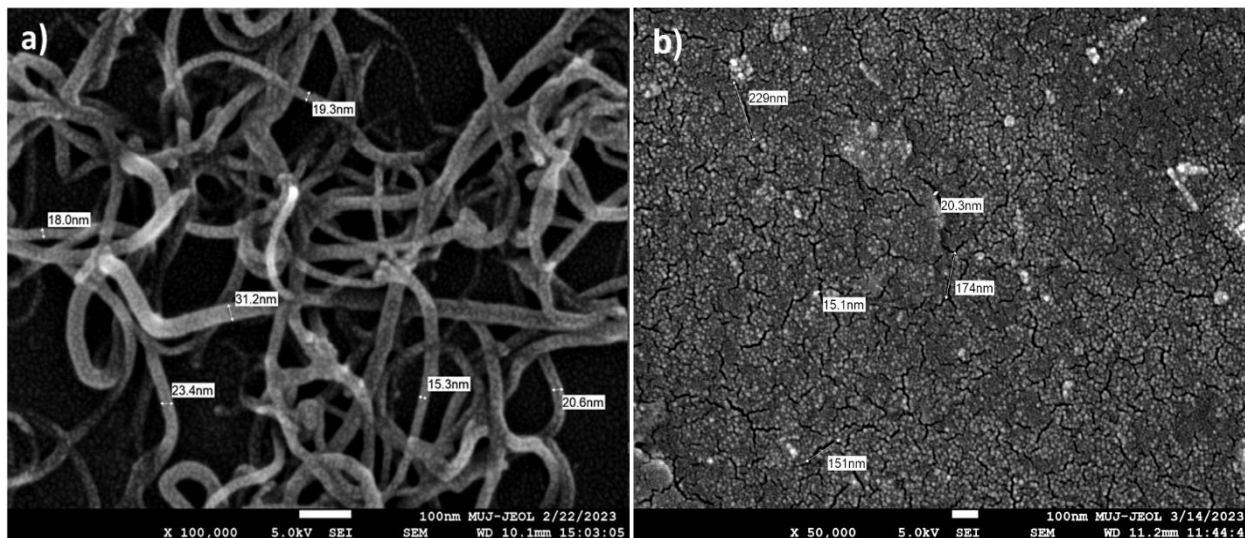*Slika 1. XRD uzorak (a) MVCNT i b) nanočestica SiO_2*

Figure 2. FESEM images of (a) MWCNT and (b) SiO₂ nanoparticles

Slika 2. FESEM slike (a) MVCNT i (b) nanočestica SiO₂

FESEM images of MWCNT and SiO$_2$ nanoparticles are shown in Fig. 2. A typical structure of MWCNT having an average diameter of 15 nm is revealed in Figure 2(a), which is found in close agreement with the result of XRD. Spherical shape SiO$_2$ nanoparticles with an average size of 15 nm is evident from the FESEM image (Fig. 2b). However, some large size clusters of nanoparticles are also revealed.

3.2. Optimization of parameters

The present work mainly focused on finding an optimum concentration of MWCNT, SiO$_2$ nanoparticles and the best curing cycle that can provide maximum tensile strength. As mentioned earlier, Taguchi DOE optimization was performed using Minitab statistical software version 18. The tensile strength, associated S/N ratio and Rank are presented in Table 3. The table reveals that the best experiment out of all is experiment 23, making hybrid sample 23 (HS23). Table 4 shows the response table of the S/N ratio. The table concludes that the curing cycle is the most influencing parameter, followed by MWCNT wt%. This is because of the fact that the curing cycle decides the level of cross linking in polymer composite. Incomplete cross linking produces a weak matrix which results in low tensile strength.

MWCNT is the most influential particle because of the fact that MWCNT can not only bridge the propagating crack but also produce a better filler matrix interface. Figure 3 shows the effect of individual variables on the tensile strength. It shows the best set of combinations is 1% MWCNT, 10% SiO$_2$ and 2nd curing cycle. Further, Regression analysis of the data was performed, and a regression equation was predicted (Eq. 3):

$$\sigma_{pr} = 73.31 + 7.22\,a + 0.717b - 5 \qquad (3)$$

where, σ_{pr} is predicted tensile strength, a is wt% of MWCNT, b is wt% of SiO$_2$, c is curing cycle number (1, 2, 3…).

The predicted value of tensile strength and associated percentage error is shown in Table 3. HS9 and HS17 showed the most deviation from the predicted value, and the same is the output from Taguchi as they ranked lower in DOE. The average % error is found to be -1.2%. Hence, the predicted model is in agreement with the actual result. The graphical representation of the same is shown in Fig. 4. Further experiments were performed to prepare hybrid epoxy nanocomposites using an optimized set of variables and results were found in close agreement with the predicted values.
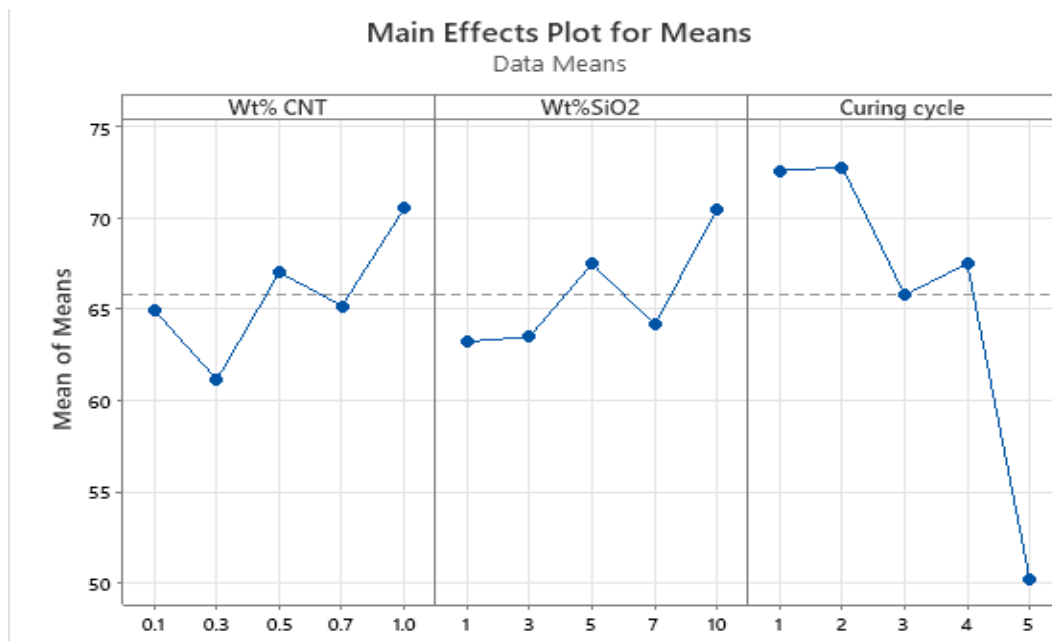
Figure 3. Effects of variables on tensile strength of HENCs

Slika 3. Efekti varijabli na zateznu čvrstoću HENC-a

Table 3. L5 orthogonal array showing value of tensile strength and associated S/N ration. (PTS = predicated tensile strength by regression analysis)

Tabela 3. L5 ortogonalni niz koji pokazuje vrednost zatezne čvrstoće i pripadajući odnos S/N. (PTS = predviđena zatezna čvrstoća regresionom analizom)

Sample No	wt% CNT	wt% SiO$_2$	Curing cycle	Tensile strength	S/N ratio	PTS (RA)	% error	Rank
HS1	0.1	1	1	69.2	36.80212	69.739	-0.779	13
HS2	0.1	3	2	78.5	37.89739	66.163	15.716	3
HS3	0.1	5	3	54	34.64788	62.587	-15.902	22
HS4	0.1	7	4	65	36.25827	59.011	9.214	17
HS5	0.1	10	5	58	35.26856	56.152	3.186	20
HS6	0.3	1	2	59	35.41704	66.173	-12.158	19
HS7	0.3	3	3	65.5	36.32483	62.597	4.432	16
HS8	0.3	5	4	70.7	36.98839	59.021	16.519	10
HS9	0.3	7	5	38	31.59567	55.445	-45.908	25
HS10	0.3	10	1	72.5	37.20676	77.636	-7.084	9
HS11	0.5	1	3	70	36.90196	62.607	10.561	12
HS12	0.5	3	4	57	35.1175	59.031	-3.563	21
HS13	0.5	5	5	59.7	35.51949	55.455	7.111	18
HS14	0.5	7	1	74.4	37.43146	76.929	-3.399	4
HS15	0.5	10	2	74	37.38463	74.07	-0.095	5
HS16	0.7	1	4	66.2	36.41716	59.041	10.814	15
HS17	0.7	3	5	43.45	32.7598	55.465	-27.652	24
HS18	0.7	5	1	73.8	37.36113	76.939	-4.253	6
HS19	0.7	7	2	73.2	37.29022	73.363	-0.223	7
HS20	0.7	10	3	69.2	36.80212	70.504	-1.884	13
HS21	1	1	5	51.7	34.26981	56.197	-8.698	23
HS22	1	3	1	73	37.26646	77.671	-6.399	8
HS23	1	5	2	79.2	37.9745	74.095	6.446	1
HS24	1	7	3	70.2	36.92674	70.519	-0.454	11
HS25	1	10	4	78.6	37.90845	67.66	13.919	2

Table 4. S/N ratio response table

Tabela 4. Tabela odgovora odnosa S/N

Level	1	2	3	4	5	Delta	Rank
wt% CNT	36.17	35.51	36.47	36.13	36.87	1.36	2
wt% SiO2	35.96	35.87	36.5	35.9	36.91	1.04	3
Curing cycle	37.21	37.19	36.32	36.54	33.88	3.33	1

1
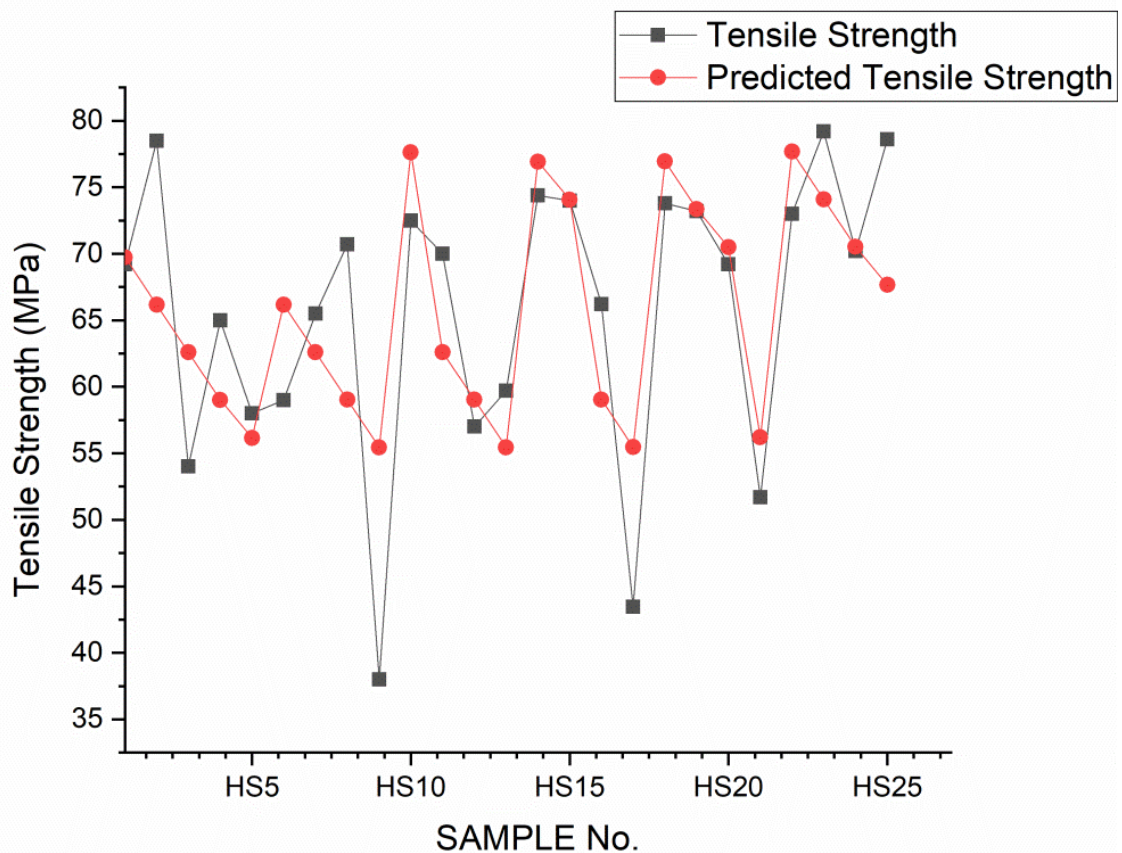
Figure 4. Tensile strength of the actual HENCs specimen v/s predicted values

Slika 4. Zatezna čvrstoća stvarnih HENCs uzorka v/s predviđenih vrednosti

3.3. Mechanical Properties

The tensile strength of base samples at three different curing cycles and hybrid samples is shown in Fig. 5(a). The tensile modulus and strain for break % of hybrid samples are shown in Fig. 5(b). The HENC HS23 demonstrated a maximum increase of approximately 13% in its tensile strength as compared to neat epoxy composite. The superior strength exhibited by the nanocomposites in contrast to the pure epoxy can be ascribed to a robust interface between the matrix and particles. This is due to the absence of any notable defects resulting from the debonding of nanoparticles, which is a common occurrence with fillers of micron scale. A robust interface facilitated a consistent transmission of stress and augmented the yield strength of the nanocomposite [32]. HENCs showed better mechanical properties compared to single particle nanocomposite (epoxy-SiO_2, epoxy-MWCNT) reported in other literature [33,34].
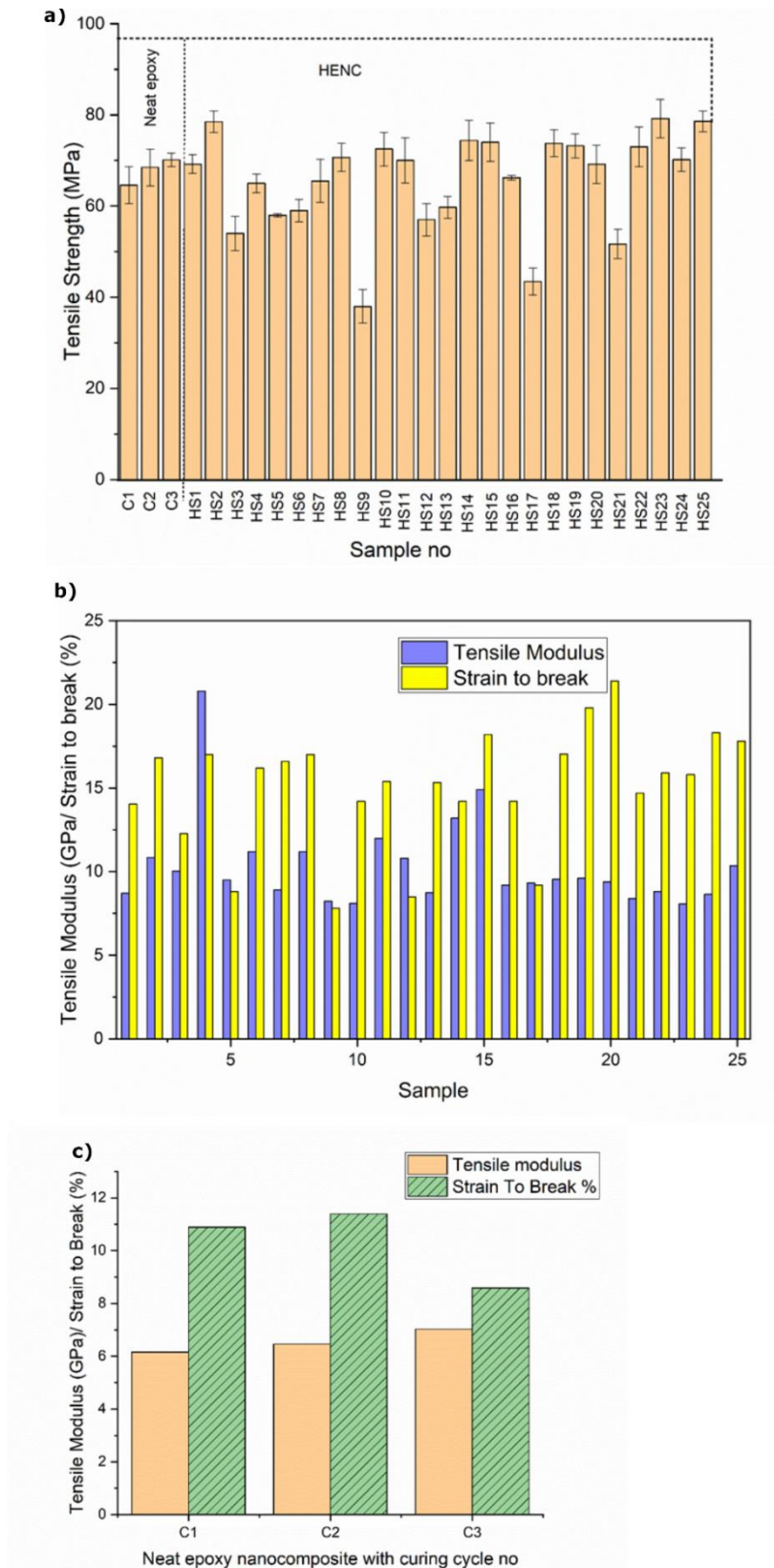
Figure 5. Mechanical properties of HENCs (a) tensile strength and (b) Strain to break % and tensile modulus. Mechanical properties of neat epoxy (c) Strain to break % and tensile modulus

Slika 5. Mehanička svojstva HENC-a (a) zatezna čvrstoća i (b) Deformacija do kidanja % i zatezni modul. Mehaničke osobine čistog epoksida (c) Deformacija na lomljenje % i modul zatezanja

HS-23 showed the best tensile strength compared to other developed HENCs. HS15 showed the best tensile modulus due to more rigidity imparted by the curing cycle. Tensile modulus and strain to break % of the HENCs demonstrated a maximum increase (compared to neat epoxy) of 200% and 81 %, respectively. Strain to break percentage is a clear indication of a decrease in brittleness. Hence, the hybrid nanocomposites show delayed cracking at a high value of strain. This may happen because of better MWCNT and matrix interaction. Adding spherical nanoparticles along with MWCNT acts as a spacer, prohibits MWCNT clustering, and results in better mechanical properties even at higher particle loading. The elevated strain-to-break % of the nanocomposite suggests the involvement of multiple failure and energy dissipation mechanisms in contrast to the composite filled with micro-particles. The enhanced modulus of the nanocomposites can be attributed to the existence of nanoparticles with high modulus. Vicker's hardness value of all samples is shown in Fig. 6. HENCs showed a maximum improvement of around 17% in hardness as compared to the base sample. HENC HS24 showed maximum hardness, i.e., 20.4 HV. Improvement in the hardness is also in agreement with the tensile strength of the HENCs. Mechanical properties of hybrid nanocomposite were found to be better than both neat epoxy and epoxy-nanoparticle nanocomposite. Further, better mechanical properties can be achieved at high particle loading in the case of HENCs.
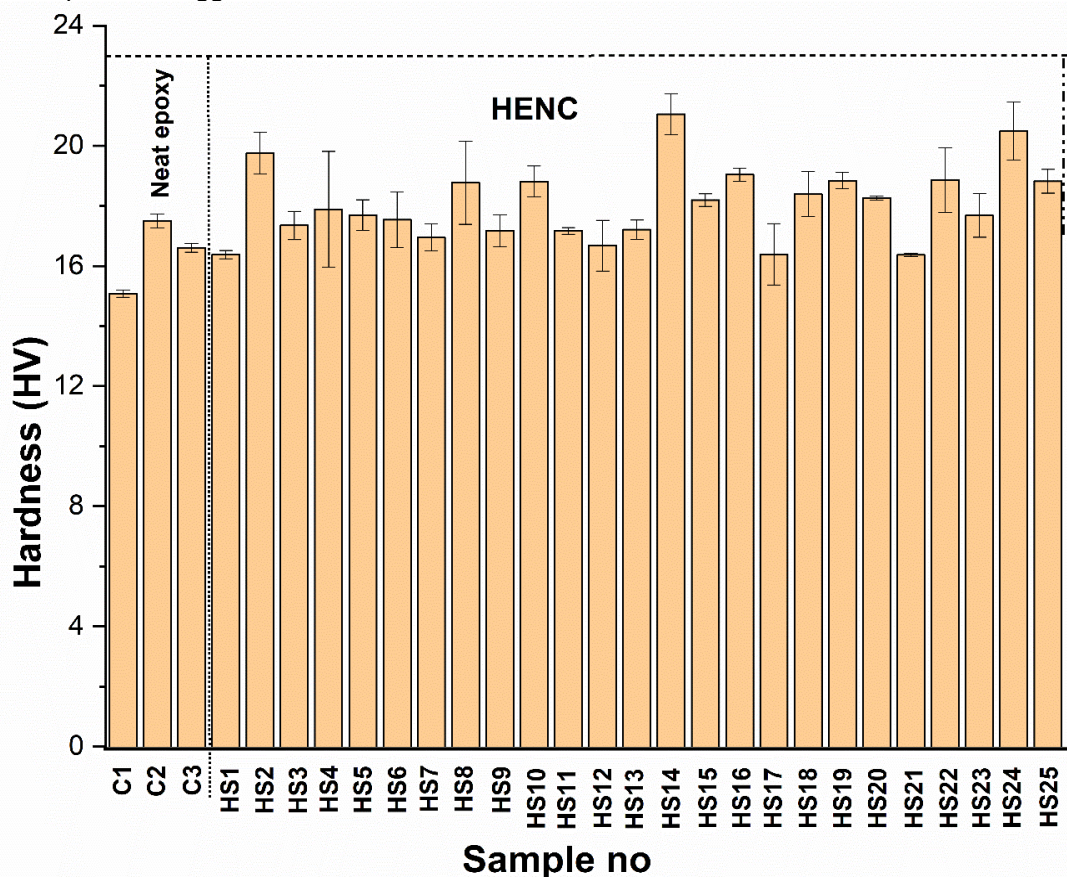

Figure 6. Hardness of neat epoxy and HENCs

Slika 6. Tvrdoća čistog epoksida i HENC-a

4. CONCLUSIONS

Taguchi design of experiments successfully optimized the concentration of MWCNT, SiO_2 nanoparticles in epoxy and curing cycle of epoxy with respect to the tensile strength of the resulting hybrid epoxy nanocomposites (HENCs). The optimal concentration of 1% MWCNT and 10% SiO_2 and curing cycle-2 revealed a noteworthy improvement in the mechanical properties of the HENCs. Tensile strength, Tensile modulus, Strain to break % and Hardness of HENCs were improved by 13%, 200%, 18% and 17%, respectively. The HENCs showed better mechanical properties compared to MWCNT/epoxy nanocomposites and SiO_2/epoxy nanocomposites because of the combined effect of both nanofillers.

This happened because SiO$_2$ nanoparticles lowered the MWCNT-MWCNT interaction and thereby reduced their agglomeration in the epoxy matrix. The homogeneously dispersed MWCNTs and SiO$_2$ nanoparticles and their threshold limit may be responsible for improved mechanical properties of HENCs.

Acknowledgements

5. REFERENCES

[1] Z.H.Zhang, Z.Y.Chen, Y.H.Tang, Y.T.Li, D.Ma, G.Zhang,... L.Tang (2022) Silicone/graphene oxide co-cross-linked aerogels with wide-temperature mechanical flexibility, super-hydrophobicity and flame resistance for exceptional thermal insulation and oil/water separation. Journal of Materials Science & Technology, *114*, 131-142.

[2] M.S.Goyat, P.Ghosh (2018) Impact of ultrasonic assisted triangular lattice like arranged dispersion of nanoparticles on physical and mechanical properties of epoxy-TiO$_2$ nanocomposites. Ultrasonics Sonochemistry, *42*, 141-154.

[3] C.Manh Vu, Q.V.Bach, L.Duong, N.Thai, V.Thao, P.Duc, T.Nguyen Van (2020) Silane coupling agent with amine group grafted nano/micro-glass fiber as novel toughener for epoxy resin: fabrication and mechanical properties. *Composite Interfaces*, *27*(12), 1085-1100.

[4] M.S.Goyat, S.Rana, S.Halder, P.K.Ghosh (2018) Facile fabrication of epoxy-6+TiO2 nanocomposites: a critical analysis of TiO2 impact on mechanical properties and toughening mechanisms. Ultrasonics sonochemistry, *40*, 861-873.

[5] D.Li, E.Peng, F.Lu, B.Wang, Y.Shen, P.Liu, Z.Hu (2023) Toughing epoxy nanocomposites with graphene-encapsulated liquid metal framework. Chemical Engineering Journal, *455*, 140887.

[6] N.Liu, H.Wang, B.Ma, B.Xu, L.Qu, D.Fang, Y.Yang (2022) Enhancing cryogenic mechanical properties of epoxy resins toughened by biscitraconimide resin. Composites Science and Technology, *220*, 109252.

[7] C.Idumah, C.Obele (2021) Understanding interfacial influence on properties of polymer nanocomposites. *Surfaces and Interfaces*, *22*, 100879.

[8] A.Kumar, S.Saini, K.Yadav, P.Ghosh, A.Rathi (2022) Morphology and tensile performance of MWCNT/TiO2-epoxy nanocomposite. *Materials Chemistry and Physics*, *277*, 125336.

[9] M.Wu, L.Lu, L.Yu, X.Yu, K.Naito, X.Qu, Q.Zhang (2020) Preparation and characterization of epoxy/alumina nanocomposites. Journal of nanoscience and nanotechnology, *20*(5), 2964-2970.

[10] K.Kumar, M.Goyat, A.Solanki, A.Kumar, R.Kant, P.Ghosh (2021) Improved mechanical performance and unique toughening mechanisms of UDM

[11] M.Al Mamun, M.A.Sabur, M.Gafur, H.Aftab, G.Rahman (2021) Fabrication and Characterization of α-Fe2O3 Nanoparticles Dispersed Epoxy Nanocomposites. Journal of Engineering Advancements, *2*(02), 95-103.

[12] A.Rathi, S.Kundalwal (2022) Synergistic effect of ultrasonically assisted exfoliated MWCNTs by ZrO2 nanoparticles on thermo-mechanical and anti-corrosive properties of epoxy nanocomposites. Journal of Composite Materials, *56*(11), 633-1649.

[13] F.Azimpour-Shishevan, H.Akbulut, M.Mohtadi-Bonab (2020) Synergetic effects of carbon nanotube and graphene addition on thermo-mechanical properties and vibrational behavior of twill carbon fiber reinforced polymer composites. Polymer Testing, *90*, 106745.

[14] D.Lee, J.Yoo, H.Kim, B.Kang, S.Park (2022) Electrical and thermal properties of carbon nanotube polymer composites with various aspect ratios. *Materials*, *15*(4), 1356.

[15] M.N.Nurazzi, M.M.Asyraf, A.Khalina, N.Abdullah, F.Sabaruddin, S.Kamarudin, S.Sapuan (2021) Fabrication, functionalization, and application of carbon nanotube-reinforced polymer composite: An overview. Polymers, *13*(7), 1047.

[16] N.Kanu, S.Bapat, H.Deodhar, E.Gupta, G.Singh, U.Vates, V.Pandey (2022) An insight into processing and properties of smart carbon nanotubes reinforced nanocomposites. Smart science, *10*(1), 40-55.

[17] A.Kumar, K.Sharma, A.Dixit (2020) Carbon nanotube-and graphene-reinforced multiphase polymeric composites: review on their properties and applications. Journal of Materials Science, *55*(7), 2682-2724.

[18] T.Yusaf, A.Mahamude, K.Farhana, W.Harun, K.Kadirgama, D.Ramasamy, H.Dhahad (2022) A comprehensive review on graphene nanoparticles: Preparation, properties, and applications. Sustainability, *14*(19), 12336.

[19] A.Díez-Pascual (2021) Chemical functionalization of carbon nanotubes with polymers: a brief overview. Macromol, *1*(2), 64-83.

[20] J.Lim, S.Bee, L.Tin Sin, C.Ratnam, Z.Abdul Hamid (2021) A review on the synthesis, properties, and utilities of functionalized carbon nanoparticles for polymer nanocomposites. Polymers, *13*(20), 3547.

[21] A.Kumar, P.Ghosh, K.Yadav, K.Kumar (2017) Thermo-mechanical and anti-corrosive properties of MWCNT/epoxy nanocomposite fabricated by innovative dispersion technique. Composites Part B: Engineering, 113, 291-299.

[22] A.Upadhyay, M.Goyat, A.Kumar (2022) A review on the effect of oxide nanoparticles, carbon nanotubes, and their hybrid structure on the toughening of epoxy nanocomposites. Journal of Materials Science, *57*(28), 13202-13232.

[23] M.Zaghloul, Zaghloul, M.Fusein (2023) Recent progress in Epoxy Nanocomposites: Corrosion, structural, flame retardancy and applications—A comprehensive review. Polymers for Advanced Technologies.

[24] S.Parihar, B.Gaur (2023) Self healing approaches in polymeric materials-an overview. Journal of Polymer Research, 30(6), 1-21.

[25] S.Wang, Y.Qiu (2022) Synthesis of SiO₂ Nanoparticle Epoxy Resin Composite and Silicone-Containing Epoxy Resin for Coatings. Applied Bionics and Biomechanics, *2022*.

[26] A.Kamel, A.Ahmed, A.El-Abd (2023) Effect of hybrid SiC/TiO2 nanoparticles on tribological and mechanical performance of polymethylmethacrylate dental base material. Zaštita materijala, 64(1), 86-95.

[27] J.He, J.Chen, L.Shi, Q.Li, W.Lu, S.Qu, G.Zhou (2019) Fabrication of thermally robust carbon nanotube (CNT)/SiO₂ composite films and their high-temperature mechanical properties. Carbon, *147*, 236-241.

[28] C.Xiao, Y.Tan, X.Yang, T.Xu, L.Wang, Z.Qi (2018) Mechanical properties and strengthening mechanism of epoxy resin reinforced with nano-SiO₂ particles and multi-walled carbon nanotubes. Chemical Physics Letters, *695*, 34-43.

[29] W.Zhou, M.Wu, Y.Wang, P.Lu, C.Wang, W.Wei, X.Miao (2023) Effect of SiO2-MWCNTs on Mechanical and Tribological Properties of Acrylic Silicone Resin Coating. Journal of Inorganic and Organometallic Polymers and Materials, 33(2), 529-543.

[30] L.Alansari, A.Diwan, S.Al-Shawi, H.Abdulsamad (2023, July) Experimental and theoretical investigating of elastic modulus of hybrid nanocomposite. In AIP Conference Proceedings (Vol. 2830, No. 1). AIP Publishing.

[31] K.Kumar, M.S.Goyat, A.Solanki, A.Kumar, R.Kant, P.Ghosh (2021) Improved mechanical performance and unique toughening mechanisms of UDM processed epoxy-SiO₂ nanocomposites. Polymer Composites, *42*(11), 6000-6009.

[32] S.Das, P.Das, S.Halder, P.Choudhury (2022) Role of Nanoreinforcement onto Intra-and Interlaminar Fracture of Hybrid Laminated Composites. In Toughened Composites (p.217-229). CRC Press.

[33] K.Bharadwaja, T.Baburao (2022) Epoxy/SiO₂ nanocomposite mechanical properties and tribological performance. Materials Today: Proceedings, *62*, 1712-1716.

[34] S.Yazman, M.Uyaner, F.Karabörk, A.Akdemir (2021) Effects of nano reinforcing/matrix interaction on chemical, thermal and mechanical properties of epoxy nanocomposites. Journal of Composite Materials, *55*(28), 4257-4272.

IZVOD

TAGUCHI DIZAJN OPTIMIZACIJE ZASNOVANE NA EKSPERIMENTIMA I EKSPERIMENTALNO ISPITIVANJE MEHANIČKIH PERFORMANSI HIBRIDNIH EPOKSIDNIH NANOKOMPOZITA

Rastuća potražnja za bezbednošću u vazduhoplovnoj i automobilskoj industriji kontinuirano motiviše istraživače da razviju lagane hibridne polimerne kompozite visoke čvrstoće, koji se obično sastoje od kombinacije ugljeničnih nanocevi (CNT) i keramičkih nanočestica u epoksidnoj matrici. Međutim, razvoj ovakvih kompozita obično ometaju neki postojeći izazovi, kao što su optimizacija koncentracije CNT-a, nanočestica i njihova distribucija u viskoznim epoksidnim matricama. Da bi se maksimalno iskoristile impresivne mehaničke karakteristike CNT-a i nanočestica SiO₂, korišćena je tehnika ultrazvučnog dvostrukog mešanja (UDM) za razvoj hibridnih epoksidnih nanokompozita (HENC) zasnovanih na MVCNT/SiO₂. Dobro poznati pristup, kao što je Taguchi dizajn eksperimenta, korišćen je za optimizaciju koncentracije MVCNT, SiO₂ nanočestica u epoksidu i ciklusa očvršćavanja epoksida u odnosu na zateznu čvrstoću nastalih HENC. Dodatno, zatezna čvrstoća, Jangov modul, deformacija do loma i tvrdoća su mereni za HENC. Rezultati su otkrili da optimalna koncentracija od 1% MVCNT i 10% SiO₂ dovodi do maksimalnog povećanja zatezne čvrstoće i drugih mehaničkih svojstava HENC-a.

Ključne reči: *hibridni nanokompozit, ultrazvučno dvostruko mešanje, optimizacija, mikromehanika, epoksid, mehanička svojstva*